Proceedings, 5th AOSFST, Newcastle, Australia, 2001
Editors: M.A. Delichatsios, B.Z. Dlugogorski and E.M. Kennedy

OBSERVATION OF EXTINCTION OF A PMMA CYLINDER FLAME WITH A FINE WATER MIST

T. Tsuruda, Liao C, and N. Saito

National Research Institute of Fire and Disaster

JAPAN

ABSTRACT

Optical observations of extinction of a PMMA cylinder flame with a fine water mist are presented. Data was obtained from a PMMA flame in a water mist stream using a particle imaging system and a particle image velocimetry system (PIV). The flow field around the PMMA cylinder was solved using the matched asymptotic theory of the Stokes approximation and the Oseen approximation. The water mist used and PMMA cylinder flame are characterized with the flux density and mass burning rate. The results show that extinction of the PMMA flame occurs before the arrival of water mist to the PMMA surface. The flux density of the water mist of 1/6 of the standard Japanese sprinkler is sufficient to extinguish the used PMMA cylinder flame. After the PMMA flame extinction, separation of water mist and PMMA surface was observed.

INTRODUCTION

Fine mist has a larger surface area per unit mass than liquid droplets. This increased surface area is expected to achieve large mass and heat transfer rates. Fine water mist extinguishers are already installed in ship board compartments. Based on this maritime application, there are a number of extinguishers for replacement of conventional ozone unfriendly gaseous extinguishers. The heat and mass transfer rates of fine mists have been studied for diesel combustion[1,2], gas turbine combustion[1,2], liquid cooling[3], and fire fighting[4]. In the 1950s and 1960s, water mist applications for fire fighting had been studied and major difficulties of this application were identified[4].

The increased surface area of water mist contributes (1) enhancement of heat and mass transfer between liquid and gas phases, and (2) increase of the viscosity effect of gas on the particle movement. In most cases, heat transfer occurs with mass transfer. In a fire situation, it is natural to expect heat transfer from fire to surroundings.

For a fine particle, the viscosity of the gas phase becomes large enough to support the particle in the surrounding fluid. If the flow velocity is large enough to support fine particles, these particles are expected to travel on the stream lines in the flow field. It is well known that stream lines do not cross each other and do not terminate in the field. This causes a serious problem to delivering water mist for protecting combustible surfaces.

In this study, optical observations of a water mist near a PMMA cylinder were carried out to verify the water mist delivery to the protecting combustible.

Background

To discuss particle movement around a protecting combustible, a set of conditions for particles and protecting combustibles are defined in Figure 1. The radius of the protecting combustible cylinder r_c, the radius of a particle r_p, and the vertical velocity of the uniform flow u are shown.

The cylindrical combustible was selected for simplification of the problem. Using the radius of the combustible cylinder r_c, the following normalised parameters[5] are introduced:

$$X = x / r_c \tag{1}$$

$$Y = y / r_c \tag{2}$$

Using the vertical velocity of the uniform flow u, the following normalised parameters are introduced:

$$V_x = v_x / u \tag{3}$$

$$V_y = v_y / u \tag{4}$$

$$T = t\, u / r_c \tag{5}$$

$$P = p / \rho u^2 \tag{6}$$

Using these parameters, normalised governing equations for incompressible, steady, and two dimensional flow are:

$$V_X\, d\, V_X / d\, X + V_y\, d\, V_X / d\, Y = -\, d\, P / d\, X + 1/R_c\, \nabla V_X \tag{7}$$

$$V_Y\, d\, V_Y / d\, X + V_Y\, d\, V_Y / d\, Y = -\, d\, P / d\, Y + 1/R_c\, \nabla V_Y \tag{8}$$

$$d\, V_x / d\, X + d\, V_Y / dY = 0 \tag{9}$$

$$R_c = \rho\, u\, r_c / \mu \tag{10}$$

ρ: density of air at 300K, 1.18 kg/m^3

μ: viscosity of air at 300K, 18.6 μPa s

The radius of the combustible cylinder and the velocity of the uniform flow u, are presumed to be 1.5 x 10^{-2} m and 0.1 m/s considering an initial stage of a normal compartment fire where a extinguisher is designed to operate.

$$R_c = 1.18 \times 1.5 \times 10^{-2} \times 0.1 / 18.6 \times 10^{-6} = 95.1 \quad (11)$$

The thickness of the boundary layer δ_c near the cylinder is estimated with following equation:

$$\delta_c = r_c R_c^{-1/2} = 1.54 \times 10^{-3} \quad (12)$$

The viscosity of the fluid affects the flow field near the cylinder surface. To discuss the particle delivery to the combustible surface, the velocity field has to be solved using the matched asymptotic theory of the Stokes approximation and the Oseen approximation. A stream function[5] for flow around a cylinder of low Reynolds number using cylindrical coordinates is:

$$\Psi = (r \log r - r / 2 + 1 / (2r)) \sin \theta / (\log (4 / R_c) - \gamma + 1 / 2) \quad (13)$$

$$\gamma = 0.577$$

where r is the non dimensional distance from the center of the cylinder, θ is the angle from the uniform flow vector. Stream lines of the stream function Ψ for R_c = 95.1 are shown in Figure 2 with normalised coordinates. X is the normalised horizontal distance from the center of the cylinder, and Y is the normalised vertical distance from the center of the cylinder.

The stream lines near the front stagnation point (0,-1) of the cylinder expand outward largely. This expansion indicates that the velocity is decreasing near (0,-1).

The stream line along the vertical center line of the cylinder intersects with the cylinder surface at (0,-1). Particles along this line will be deposited on the cylinder surface.

Stream lines at the horizontal center line $Y = 0$ of the cylinder are parallel with the cylinder surface. This fact shows that no particle is moving toward the cylinder surface at $Y = 0$.

Separations between stream lines become small at the horizontal center line $Y = 0$. This decreased separation shows that the velocity is increasing near $Y = 0$.

The drag[5] with presumed particle radius r_p = 15 μm is:

$$D = 24 / (u_p r_p \rho / \mu) \pi r_p^2 (\rho u_p^2 / 2) = 12 \mu \pi r_p u_p \quad (14)$$

In steady state, the weight of a particle is equal to the drag induced by it falling in the fluid with the velocity u_p. Assuming that the weight of the air is negligible, the weight of a particle is:

$$m = 4/3 \pi r_p^3 \rho_p \quad (15)$$

Balancing the gravitational force and the drag working on the particle, the next equations are obtained:

$$12 \mu \pi r_p u_p = m g = 4/3 \pi r_p^3 \rho_p g \quad (16)$$

where ρ_p is the density of water at 300 K (998 kg/m^3) and g is the gravitational acceleration (9.8 m/s^2).

$$u_p = 1.31 \times 10^{-2} \quad (17)$$

Thus, the particle is moving in the fluid at 1.31 x 10^{-2} m/s. This particle is slipping 13 % with respect to the fluid velocity.

EXPERIMENTAL SETUP

Particle imaging system

Figure 3 shows a schematic top view of the particle imaging system. The system consisted of two parts: an optical illuminator; and a high speed video camera. The illuminator employed a 1 kW Xenon lamp as shown in Figure 3. A concave mirror focused a pinhole image on a beam stop. The beam stop covered one quarter of the lens of the high-speed video camera. An 85 mm F 1.4 lens focused scattered light on the CCD of the high-speed video camera. Only particles and edges of transparent objects appeared as bright areas. A series of 512 images of 512 x 480 size were recorded with a 1/10000-second exposure time. A digital video recorder acquired recorded images. Image processing was performed on a PC.

Particle image velocimetry system (PIV)

Figure 4 shows a schematic side view of the particle image velocimetry system (TSI). The system consisted of two parts: a Nd: YAG laser; and a CCD camera. A synchronizer triggered a Nd:YAG laser of 280 mW at 15 Hz. A lightsheet optics produced fan shaped beam. A zoom-micro lens (AF Zoom-Micro Nikkor ED 70-180 mm F 4.5-5.6, Nikon) focused scattered light on the CCD of the camera. A series of 110 image pairs of 1000 x 1016 size were recorded. Recorded images were acquired by a PC workstation, equipped with a frame grabber board and an image processing software.

Mist generator

The mist generator used in this study was a humidifier (TDK PTC Humidifier KS-520G) which generated water mist by boiling water with an electric heater. The mist generator had an 80 mm diameter circular opening on the top cover. The total water evapouration rate was 4 g/minute. The mean water flux density at the opening was 1.33×10^{-5} g/(s mm^2). The temperature of the generated mist was 48 - 53^{0}C at 100 mm above the opening of the mist generator. The saturated vapour pressure of water at 50^{0}C is 1.23×10^{-2} Mpa[7]. A metal plate was used to block the water mist for the free burning of the PMMA cylinder.

PMMA cylinder

The PMMA cylinder used in this study was a 30 mm long block, 30 mm in diameter. The PMMA cylinder was supported with a stainless tube of 9.9 mm in diameter. The PMMA cylinder was mounted horizontally. The center axis of the cylinder was 90 mm above the opening of the mist generator.

The mass of the PMMA cylinder was measured with a balance. The mass burning rate of the PMMA cylinder after 60 s burning was 3.8×10^{-2} g/s.

EXPERIMETAL RESULTS

Experimental procedure

A PMMA cylinder was mounted above the mist generator. The optical elements were adjusted to produce a clear particle image. A shutter of metal plate covered the opening of the mist generator. Droplets on the PMMA cylinder were wiped off with a sheet of paper. The behaviours of the particles around the PMMA cylinder were recorded after removing the shutter. The recorded images were stored on disks and tapes.

High-speed images

Figure 5 shows a series of high-speed particle images around a PMMA cylinder without flame. Images are shown in negative to improve water mist imaging. The size of each frame was 9.5 x 8.8 mm. The frame rate was 250 frames/s. The time, *t*, after the water mist arrival at the cylinder surface, is shown. At t = -32 ms, water mist is seen 5 mm below the cylinder surface. After t = -32 ms, water mist was travelling upward with a constant velocity. The mean velocity of the leading edge of the water mist was 1.48×10^{-1} m/s.

Figure 6 shows a series of high-speed particle images around a PMMA cylinder with flame. At t = -36 ms, water mist was seen near the bottom of the frame. A triangle shape image was seen under the cylinder. At t = -20 ms, the left end of the triangle shaped image expanded to the left side and up ward. At t = -12 ms, the left end of the triangle shape contacts with the cylinder surface. Below this triangle area, water mist is seen clearly. From t = -12 ms to 0 ms, the surface shape of the cylinder was changing with forming dips. After t = 0 ms, the surface of the cylinder expanded downward. The flame was extinguished instantly after removing the shutter.

PIV images

Figure 7 shows a series of PIV images around a PMMA cylinder without flame. The size of each frame was 65 x 64 mm. Images are shown in negative to improve water mist imaging. The frame rate was 15 frames/second. A vertical laser sheet was crossing the middle of the axes of the PMMA cylinder. The water mist of the left side of the PMMA cylinder was not seen in the frame at t = 0 because the illuminating laser was blocked by the PMMA cylinder. Due to the high spatial resolution of the CCD camera and a 300 μ m slit, water mist was resolved to particles. The presence of water particles on the PMMA cylinder surface was seen in the frame at t = 0 ms.

Figure 8 shows a series of PIV images around a PMMA cylinder with flame. At t = -133 ms, a smooth leading edge of water mist is seen with flame around the PMMA cylinder. The separation between the PMMA cylinder and flame was 2.2 mm in this frame. At t = -67 ms, a small flame below the PMMA cylinder is seen with 5 mm separation from the leading edge of water mist. The leading edge of water mist was deformed along the PMMA cylinder surface. A spike shape of water mist is seen on the right side of the PMMA cylinder. This spike indicates the presence of a high-speed region near the PMMA cylinder surface. At t = 0 ms, no flame is seen in the lower part of the PMMA cylinder. In this frame, the separation between the PMMA cylinder and leading edge of water mist is 2 mm.

DISCUSSION

Extinction of PMMA cylinder flame

A PMMA cylinder flame was extinguished with a water mist with a flux density of 1.33×10^{-5} g/(s mm^2) in this study. The water discharge rate of the standard Japanese sprinkler is 80 L/min for a 2.3 m cover radius. The mean flux density of the standard Japanese sprinkler is 8.03×10^{-5} g/(s mm^2). A kerosene fire of 200 mm in diameter is extinguished with water mists of the flux density of 1×10^{-4} g/(s mm^2) in 2 seconds[4]. The flux density in this study was 1/6 to 1/7.5 of these flux densities. Extinction of the PMMA cylinder flame occurs within 1 second after removing the shutter. The mean traveling time of water mist from the opening to the PMMA cylinder was about 0.6 seconds. The extinction of the PMMA cylinder flame occurred after the arrival of water mist.

Behaviour of water mist near PMMA cylinder without flame

As shown in Figure 7, particles of water mist are delivered to the PMMA cylinder surface. The delivered particles deposit on the PMMA cylinder surface in this study. The PMMA cylinder surface at room temperature seems to be cooling the used hot water mist. If water is transported to the cold surface by condensation, the total water flux becomes much larger than that transported by convection.

Behaviour of water mist near PMMA cylinder with flame

As shown in Figures 6 and 8, the extinction of the PMMA cylinder flame occurs before the contact of water mist and PMMA surface. The surface temperature of burning PMMA is more than 600K[(8)]. The forming temperature is reported to be about 400K[(8)]. The condensation of decomposed PMMA gas is considered to occur near the forming temperature. In this study, a PMMA flame was cooled with approaching water mist whose temperature was less than 100^0C under normal pressure. It is expected that the decomposed PMMA gas is cooled by water mist. The triangle shape area in Figure 6 seems to be the condensed particles of decomposed PMMA gas. The forming of condensed particles indicates that the heat release rate at the flame zone is lowered by the water mist arrival near the flame.

The separation between the water mist and extinguished PMMA surface indicates decomposed PMMA gas pushing back from the surface. The generation of decomposed PMMA gas seems to continue until surface expansion of the PMMA, which is driven by gas accumulation in the molten PMMA.

Diameter of particles of water mist

In this study, the diameter of the water mist was not directly measured. The particle image of the used water mist was observed with magnification optics. The maximum particle diameter was estimated less than 30 μm. If there is a particle of 60 μm diameter, the terminal velocity of the particle is 5.24×10^{-2} m/s which is 35 % of the velocity of the leading edge of water mist.

CONCLUSIONS

This study demonstrated detailed flame extinction and particle behaviour around a PMMA cylinder. The experiments revealed:

1. The extinction of a PMMA cylinder flame occurs before the contact of water mist with the PMMA surface.

2. A water mist flux density of 1.33×10^{-5} g/(s.mm^2) is sufficient to extinguish a PMMA cylinder flame. This flux density is equivalent to 1/6th of the water discharge rate of a standard Japanese sprinkler.

3. The deposition of water droplets was observed on the PMMA cylinder surface without flame.

4. The separation between the water mist and extinguished PMMA was observed. The stagnation surface seems to be formed by the ejection of decomposed PMMA gas from the extinguished surface.

REFERENCES

1. Kumagai, S., Combustion of Fuel Sprays, Sixth Symposium(International) on Combustion, pp.668-674, Reinhold Publishing Corporation,1956.

2. Isoda, H. and Kumagai, S., New Aspects of Droplet Combustion, Seventh Symposium(International) on Combustion, pp.523-531, Butterworths Scientific Publications, 1958.

3. Tamura, Z. and Tanagawa, Y., Evaporation and Combustion of a Drop Contacting with a Hot Surface, Seventh Symposium(International) on Combustion, pp.509-522, Butterworths Scientific Publications, 1958.

4. Yaji, Y., Study on Extinguishment of Fire by Spray (2nd Report), pp.21-25, Bull. of The Fire Prevention Society of Japan Vol.11, No.1, 1961.

5. Kida, S., Introduction of fluid-flow problems, pp.66-96, Kyouritsu, 1994.

6. Schlichting, H., Boundary-Layer Theory, McGraw-Hill, 1979.

7. JSME, JSME Mechanical Engineers' Handbook A. Fundamentals A6: Thermal Engineering, pp.49-50, Mruzen 1985.

8. Olson, S. L., and T'ien, J. S., Buoyant Low-Stretch Diffusion Flames Beneath Cylindrical PMMA Samples, pp.439-452, Combustion and Flame 121, 2000.

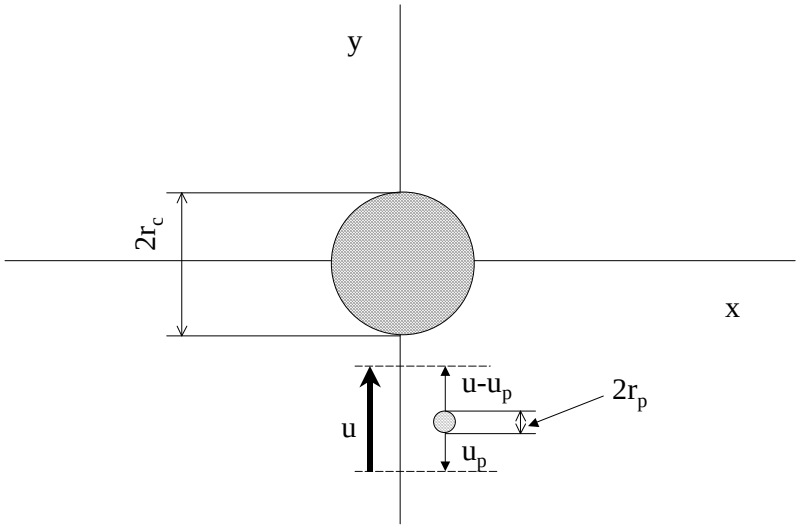

Figure 1: Particle and protecting combustible.

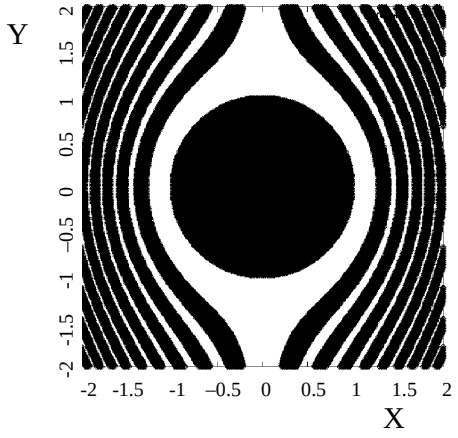

Figure 2: Streamlines.

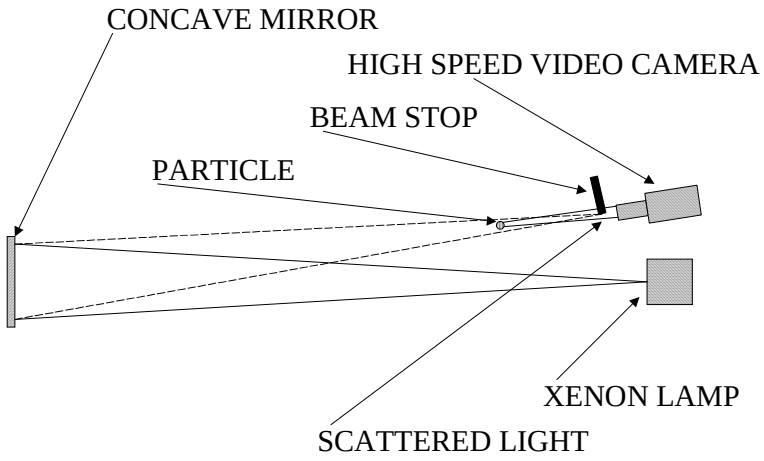

Figure 3: Schematic of the particle imaging system.

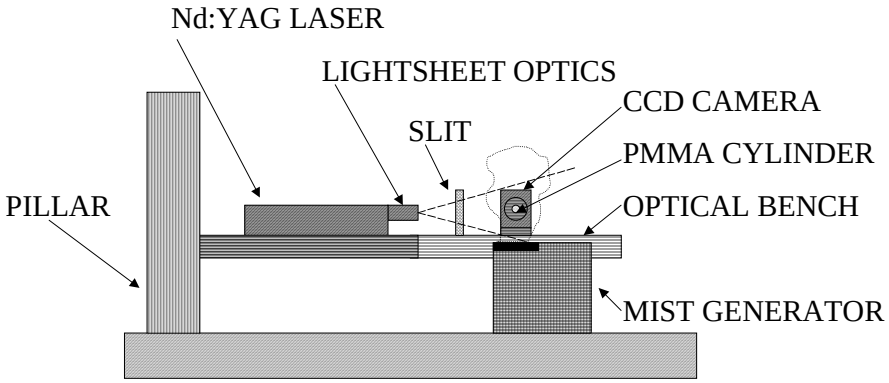

Figure 4: Schematic side view of the particle image velocimetry system.

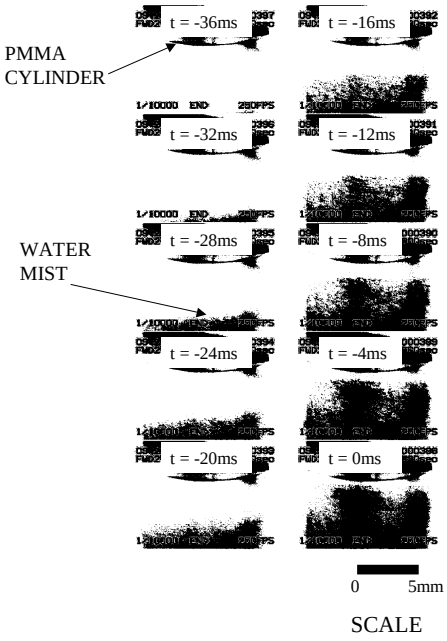

Figure 5: A PMMA cylinder without flame.

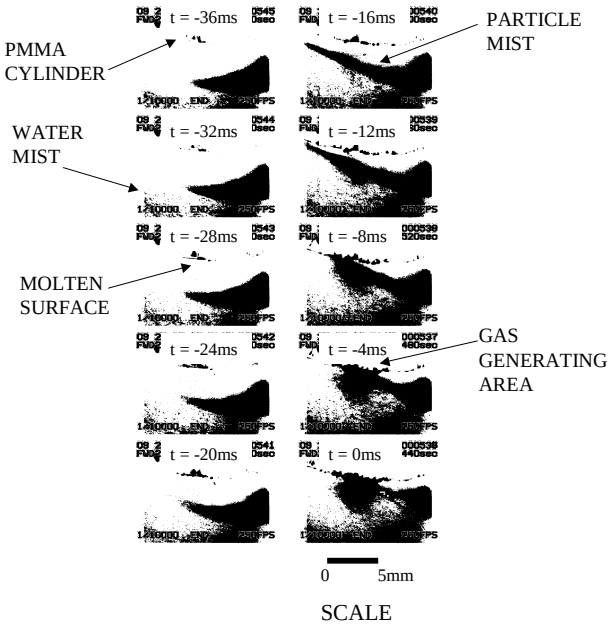

Figure 6: A PMMA cylinder with flame.

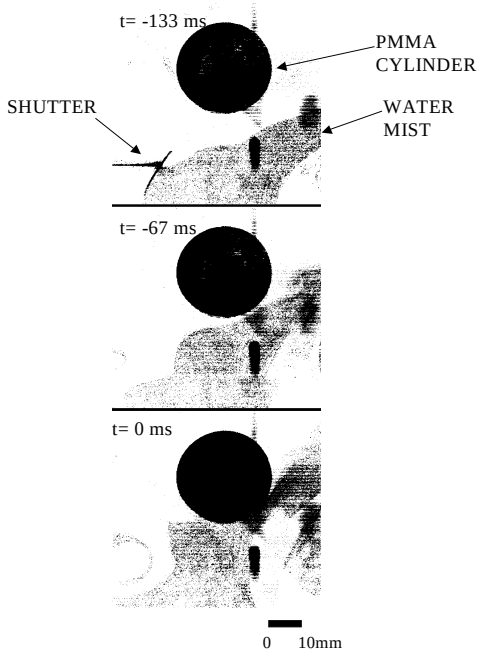

Figure 7: PIV images without flame.

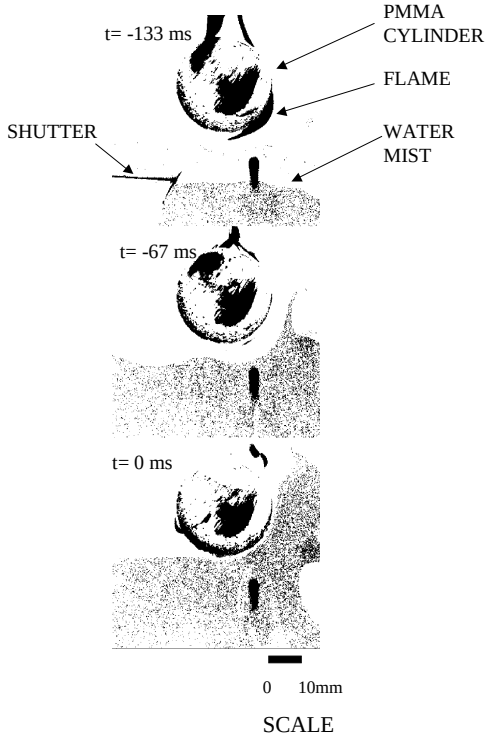

Figure 8: PIV images with flame.